

# Wearable Textile Fabric Based 3D Metamaterials Absorber in X-Band

E. Delihasanlar and A. H. Yuzer

Department of Electrical-Electronics Engineering  
Karabuk University, Karabuk, 78050, Turkey  
edizdelihasanlar@karabuk.edu.tr, hayrettinyuzer@karabuk.edu.tr

**Abstract** — In this paper, a new wearable (flexible) textile fabric-based 3D metamaterials absorber (MMA) structure is proposed. The proposed MMA was created from three layers; weft-knitted fabric, silicone, and plain weave fabric and then, it was simulated in Computer Simulation Technology (CST). It was obtained maximum absorption power (99.66%) at 9.38 GHz, and the average absorption power of 81-95% was obtained in the frequency range of 8 to 12 GHz depending on the incident angle in the simulation. The effect of the wearable textile structure on absorption was investigated. When compared with other materials, it can be said that the proposed MMA is broadband, incident angle independent, TE and TM polarization-independent, flexible, breathable, wearable, ease of fabrication, practical, low weight, and cost advantage. With this designed the textile fabric-based MMA, it can be obtained both low reflection coefficients and low transmission coefficients at broadband X-band frequencies. This provides a good solution for the cloaking of radar systems.

**Index Terms** — 3D metamaterial, cloaking, plain weave, textile, wearable absorber, weft-knitted.

## I. INTRODUCTION

Metamaterials, which is not found in nature, is an artificial material having extraordinary features. The material has negative dielectric permeability ( $\epsilon$ ) and negative magnetic permeability ( $\mu$ ) in the special frequency range. Metamaterials can be adapted to the desired range in the electromagnetic spectrum according to the application areas. It has a wide potential application in many areas such as electromagnetic cloaking [1-2], superlens [3-4], sensing [5], absorber [6-9], the antenna [10-17], etc. [18-20].

Metamaterial periodic resonator shapes are on the order of a wavelength of incident electromagnetic waves. When the EM wave arrives at the metamaterial structure, the periodic resonator will generate a surface current that causes electrical resonance. The periodic resonator layer and the conductive layer will generate reverse current to the surface current. This will cause magnetic resonance.

If the electrical and magnetic resonance are obtained at the same bandwidth, the perfect absorber is obtained [21-22]. The transmission and reflection coefficients depend on the MMA. If the intrinsic impedance of the medium and MMA are matched, the incident wave will not be reflected and will be absorbed perfectly as dielectric losses. Typically, MMA is fabricated on rigid [21, 23] and flexible [6] materials depending on the application. Recent studies have been focused on flexible MMA that can be easily integrated application. Many materials have been used to get flexible MMA designs, for example polydimethylsiloxane [24], polymer [25-26], polyimide [27-31], silicone [32], polypropylene [33], composite [34], and textile [3, 35-39]. The advantage of the textile, compared to other materials is flexibility, breathability, wearable, ease of fabrication, practicability, low weight and cost. In the literature, there are many works on textile-based MMA applications. In these works, periodic shapes were made by using sticking techniques on textiles. It was created by using the screen-printing [22], inkjet printing [24, 40], lithographic processes [25], and stamping [26] techniques. It is not found an application at which 3D textile geometry was used for designing textile-based MMA.

In this study, a 3D textile fabric-based MMA was designated for the X-band frequency range (8-12 GHz) in the CST simulation. The MMA consists of the periodic resonator shapes, a conductive layer, and a dielectric substrate. The weft-knitted fabric and plain weave fabric was used as periodic resonator shapes and the conductive layer, respectively. The 3D periodic resonator shapes were obtained by forming copper in the half-loop of weft-knitted fabric. Details of the usage of plain weave fabric structure as a conductive layer are given in the [41]. The flexible 1.6 mm thick silicone dielectric layer was used to combine the periodic resonator shapes with the conductive layer to improve the absorption performance. The simulation measurements were performed in the range of 8-12 GHz (X-Band), where many communication systems operate. The incident angle and the polarization effect were investigated. 99.66% of the highest absorption was observed at TM polarization with 0° incident angle at

9.38 GHz. The average absorption power of MMA is swinging between 81% to 95% depending on the incident angle. Moreover, the effect of the wearable textile structure on absorption was investigated by using the scaling method in the CST simulation program. The major difference of the designed material from the previously published studies is that it is not only the 3D wearable textile structure but also it provides high absorption in wideband and is independent of incident angle and polarization [35-39]. Designed MMA can be used in commercial, communication and military defense application.

The outline of this study is as follows. It was introduced the theory, preparation, and simulation of textile-based MMA in Section II. Next, the incident angle effect, the polarization effect, the scaling effect on the absorption power of the designed MMA were given in Section III. Finally, it was described how to use MMA of results and was drawn future works in Section IV.

## II. MATERIALS AND METHODS

Materials complex permittivity and complex permeability properties depend on the frequency. When a perfect absorbent is wanted to design, the imaginary parts of dielectric materials are also very important because they add extra dielectric loss. If the intrinsic impedance of the medium and materials impedance can be matched, incident electromagnetic waves will not be reflected. Many researchers have been working intensively on impedance matching and dielectric loss with MMA.

MMA structures consist of three layers, which are periodic resonator shapes, a conductive layer, and a dielectric substrate. The periodic resonator shape resonates with the incident electromagnetic waves as its size is smaller than the wavelength of the incident electromagnetic waves. The periodic resonator shape and conductive layer were adapted to the textile structure to form the MMA structure. To create 3D periodic resonator shapes, a weft-knitted fabric structure having a wide range of the loop was used. Since the loop of plain weave fabric is very smaller than the measured wavelength, it behaves like a conductive surface. The silicone material was used to form a flexible structure. It keeps the two fabrics fixed and create a high dielectric loss.

The absorption power of materials can be calculated from the reflection coefficient and the transmission coefficients of the medium. Total reflection coefficients and transmission coefficients can be explained by using the multiple reflections theory [42]. The first interface medium reflects part of the incident electromagnetic wave and transmits the other part of the incident electromagnetic waves. The end interface reflects and transmits a portion of the waves transmitted from the first interface. This event continues until the wave

disappears in the lossy medium. Illustration and mathematical representation of this phenomenon are given in Fig. 1. The total reflections coefficient,  $S_{11}$ , is written as a function of frequency as given in (1):

$$\begin{aligned} \Gamma_1(\omega) &= \rho_1 + \sum_{n=1}^{\infty} \tau_1 \tau_1' (\rho_1')^{n-1} \rho_2^n e^{-j\omega n T}, \\ R(\omega) &= \Gamma_1(\omega)^2 = |S_{11}|^2, \end{aligned} \quad (1)$$

where  $R(\omega)$  represents the reflection coefficient.

The total transmission coefficients,  $S_{21}$ , are written as a function as given in (2):

$$\begin{aligned} T(\omega) &= \sum_{n=1}^{\infty} \tau_1 \tau_2 (\rho_1')^n \rho_2^n e^{-j\omega n T} e^{-j\omega T/2}, \\ T(\omega) &= |S_{21}|^2. \end{aligned} \quad (2)$$

The absorption power of materials is calculated by using the equation given in (3):

$$A(\omega) = 1 - T(\omega) - R(\omega) = 1 - |S_{11}|^2 - |S_{21}|^2. \quad (3)$$

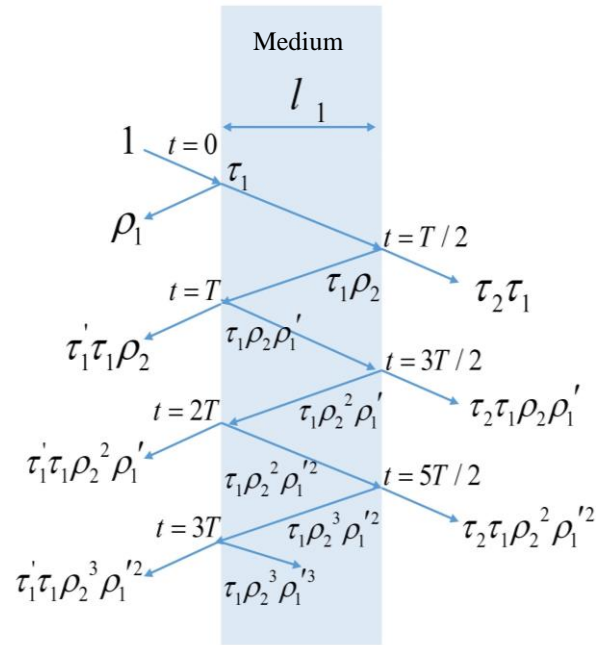


Fig. 1. Multiple reflections theory.

### A. Material properties of the knitted and woven fabrics

Weft-knitted fabric is one of the basic knitting fabric structures. Wales and course density construct its horizontal pattern and vertical pattern, respectively [43].

Plain weave fabric has the simplest structure among woven fabrics. It consists of the weft and warp yarns woven together that are knitted one after another. When the cotton yarn is taken from the conductive yarn that forms the fabric, the only metal mesh will leave. Hence, the physical structure of the composite plain weave fabric is similar to metal mesh. Many analytical solutions have been derived from this type of structure [44]. The weft-knitted and plain weave fabrics properties are given in Table 1.

Table 1: Fabric properties

	Copper Content (%)	Yarn (nm)	Knitting Density		Weaving Density	
			Wales (1/10 cm)	Courses (Loops/cm)	Warp (Tread/cm)	Weft (Tread/cm)
Weft-Knitted	5.5	7.06	50	3	-	-
Plain Weave	11	7.06	-	-	10	10

### B. Metamaterials based textile design

The weft-knitted and the plain weave fabric structures are designed by using computer-aided design software (AutoCAD). The designed half-loop periodic copper structure was applied to the drawn geometry of weft-knitted fabric. Then it was included in the entire loop structure. The plain weave fabric structure was created as full copper. In the designs, the yarn thickness was as 50  $\mu\text{m}$  and the dielectric constant of the textile yarn was neglected. The designed textile fabrics were imported into the CST program for simulation.

The designed 3D half-loop periodic copper weft-knitted structure is shown in Fig. 2. The designed copper plain weave fabric structure is presented in Fig. 3. Silicone was used as the dielectric substrate. The thickness of the material was 1.6 mm. The silicone material properties in the CST program were given in Table 2.

Table 2: Silicone properties

<b>Epsilon (<math>\epsilon</math>)</b>	11.9
<b>Mue (<math>\mu</math>)</b>	1
<b>Electrical Conductivity</b>	0.00025 S/m
<b>Material Density (Rho)</b>	2330 Kg/m <sup>3</sup>
<b>Thermal Conductivity</b>	148 W/K/m
<b>Heat Capacity</b>	0.7 kj/K/kg

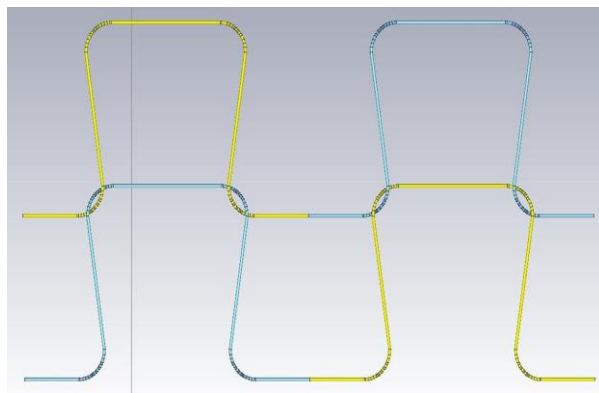


Fig. 2. Weft-knitted fabric with half loop copper structure.

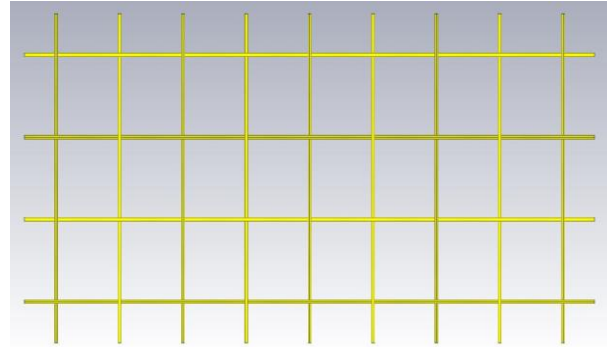


Fig. 3. The copper plain weave fabric structure.

One-unit 3D half-loop periodic copper weft-knitted fabric structure dimensions were given in Fig. 4 (a). The 3D side view was given in Fig. 4 (b). One-unit copper plain weave fabric structure dimensions were given in Fig. 4 (c). The 3D side view was given in Fig. 4 (d).

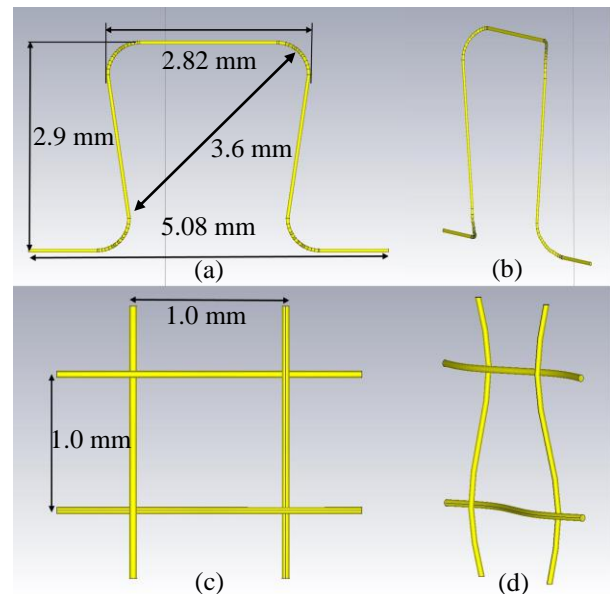


Fig. 4. (a) One-unit half-loop copper weft-knitted fabric dimension, (b) one-unit half-loop copper weft-knitted fabric side view, (c) one-unit copper plain weave fabric structure dimension, and (d) one-unit copper plain weave fabric side view.

### C. Simulation setup

The MMA was formed by combining weft-knitted fabric, silicone and plain weave fabric. It is given in Fig. 5. Front view of the weft-knitted fabric (a), side view of the weft-knitted fabric (b), rear view of the plain weave fabric(c), and side view of the plain weave fabric (d). The total thickness of the textile-based MMA is 2.23 mm. The weft-knitted fabric, silicone, and plain woven

fabric thicknesses are 0.38 mm, 1.6 mm, and 0.25 mm, respectively.

The 2-port waveguide measurement system was created in the CST simulation program to investigate the absorption power of MMA at 8-12 GHz frequency range. A full mesh cell MMA is simulated in the CST program by using the finite-difference time-domain (FDTD) method. The full mesh cell MMA size was defined as 10×10 cm. The defined physical properties of the surrounding space were selected as “normal”. Boundary conditions were selected according to the polarization mode (TE, TM). The waveguide simulation setup is shown in Fig. 6. The MMA was rotated on the axis by the specified angle to investigate the incidence angle dependence.

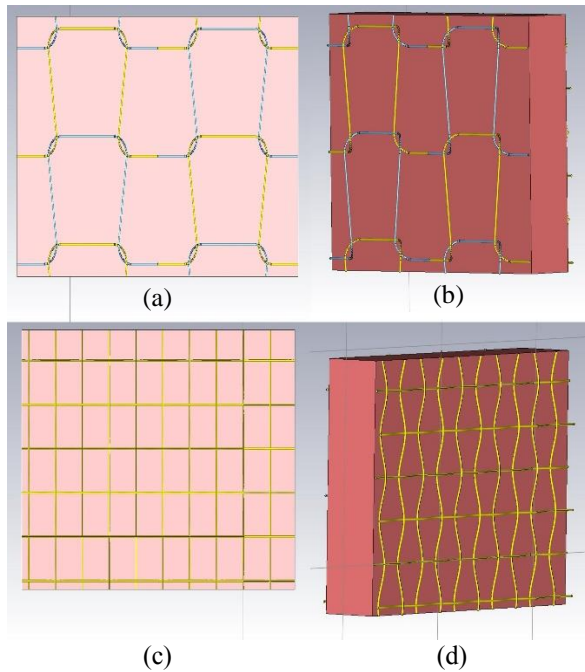


Fig. 5. (a) Front view of the weft-knitted fabric, (b) side view of the weft-knitted fabric, (c) rear view of the plain weave fabric, and (d) side view of the plain weave fabric.

### III. RESULTS AND DISCUSSION

The absorption power of materials was calculated by using S parameters. Polarizations (TM and TE) and incident angles (-20° to 20°) effects on absorption are investigated in the measurements. Besides, the absorption power of MMA was investigated by forming an MMA structure with a just dielectric substrate (silicone) without copper to reveal the MMA structure effect. The effect of silicone on the absorption power of MMA without copper is also given in Fig. 7 and Fig. 8.

Figure 7 shows the result of the absorption power of MMA at TM polarization within the 8-12 GHz frequency range and gives the effect of incident angles on

absorption. The maximum and average absorption power of MMA are also given on the same figure.

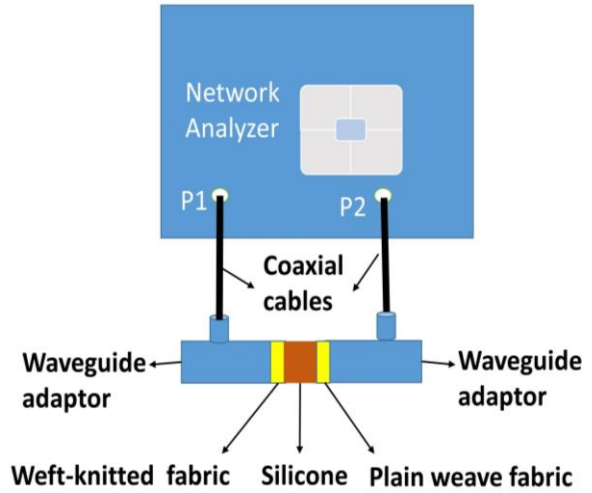


Fig. 6. Waveguide simulation setup.

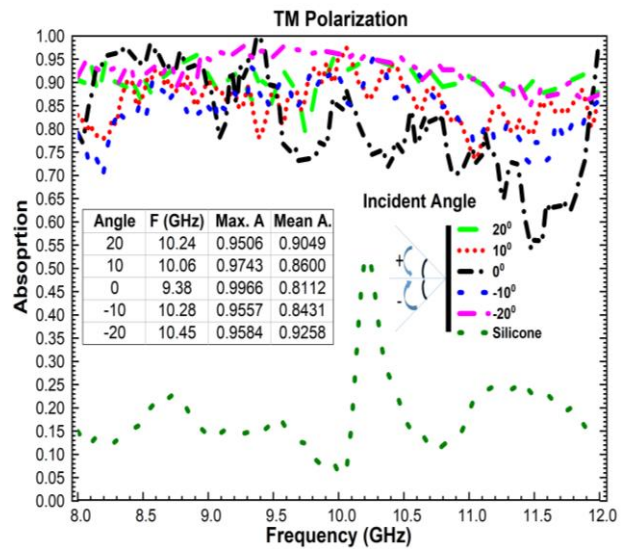


Fig. 7. Absorption power at TM polarization.

Figure 8 shows the result of the absorption power of MMA at TE polarization within the 8-12 GHz frequency range and gives the effect of incident angles on absorption. The maximum and average absorption power of MMA are also given on the same figure.

Ideally, a perfect absorber should have very low transmission coefficients and a reflection coefficient. The maximum absorption power (99.66%) was obtained at TM polarization with 0° incident angle at 9.38 GHz. As the angle increases, the cross-sectional area of the periodic shape becomes smaller. This causes the maximum absorption power of MMA occurred at a higher frequency. The average absorption power of

MMA is swinging between 81% to 95% depending on the incident angle. The designed MMA achieved high absorption power in wideband. It can be said that the absorption power of MMA is almost independent of incident angle and polarization.

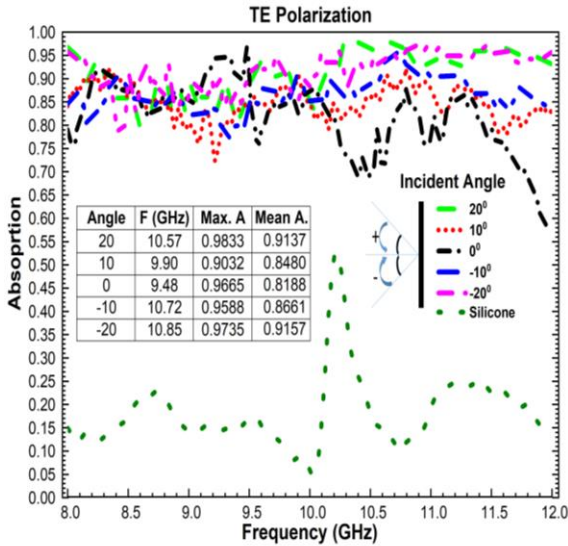


Fig. 8. Absorption power at TE polarization.

Other simulations were performed to investigate the effect of flatness, flexibility, compression, and folding of the structure in the CST program. In these situations, the textile loop size is changing. Thus, the dimension of the textile structure was scaled to investigate the effect of these situations on absorption. The whole textile-based MMA structure was scaled by -10%, -5%, 0%, 5%, and 10% at TE polarization with +20° incident angle and simulations were performed. The maximum absorption resonance frequency is shifted, and the average amount of absorption is gradually increased. The results are given in Fig. 9.

#### IV. CONCLUSION

The textile-based MMA design operating at the X-band was demonstrated in the CST simulation program. The absorption power of MMA was calculated by using the transmission coefficient and the reflection coefficient. The maximum absorption power (99.66%) was obtained at TM polarization with 0° incident angle at 9.38 GHz. The average absorption power of MMA is swinging between 81% to 95% at 8-12 GHz frequency band depending on the incident angle. It was found that the angle of the incident and the polarization type of electromagnetic waves did not affect the absorption power of MMA. Initially, it was aimed to design the MMA absorbing at 8-12 GHz. In the incident angles simulation results, absorption was as expected at 8-11 GHz. However, the same performance could not be

achieved at high frequencies ( $11 \text{ GHz} < f < 12 \text{ GHz}$ ) for normal incidence. When the angle of incidence was increased, the cross-sectional area would be decreased, therefore better results were obtained for angular incidence. The proposed MMA was scaled to investigate the effect of wearable textile structure on absorption, too. As a result of scaling, the maximum absorption frequency is shifted, and the average absorption is a bit increased. It was found that wearability did not have a remarkable effect on absorption.

The optimum production process is under process. When the best production technique is determined, MMA will be produced. The proposed MMA can be used to prevent the detection of soldiers and military equipment from radar. Also, this proposed MMA can be used as an anechoic chamber for X-band applications.

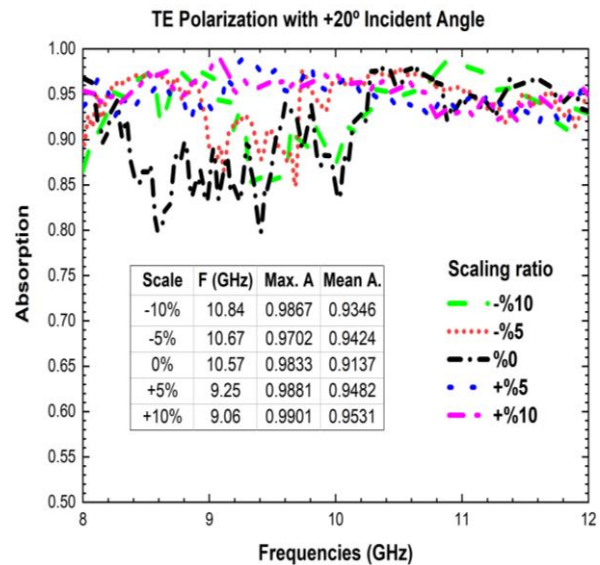


Fig. 9. The scaling effect results.

#### REFERENCES

- [1] B. Greinke, M. Candotti, A. Alomainy, and C. Parini, "Parameters extraction of three-dimensional structures for graded textile cloaking materials," *2013 Loughbrgh. Antennas Propag. Conf. LAPC 2013*, pp. 84-87, Nov. 2013.
- [2] T. Zhang, *et al.*, "Tunable plasmon induced transparency in a metallodielectric grating coupled with graphene metamaterials," *J. Light. Technol.*, vol. 35, no. 23, pp. 5142-5149, 2017.
- [3] M. Esen, I. Ilhan, M. Karaaslan, E. Unal, F. Dincer, and C. Sabah, "Electromagnetic absorbance properties of a textile material coated using filtered arc-physical vapor deposition method," *J. Ind. Text.*, vol. 45, no. 2, pp. 298-309, 2015.
- [4] Y. Tao, E. Yang, and G. Wang, "Left-handed metamaterial lens applicator with built-in cooling feature for superficial tumor hyperthermia," *Appl.*

- Comput. Electromagn. Soc. J.*, vol. 32, no. 11, pp. 1029-1034, 2017.
- [5] M. Bakır, M. Karaaslan, F. Karadag, S. Dalgac, E. Ünal, and O. Akgöl, "Metamaterial sensor for transformer oil, and microfluidics," *Appl. Comput. Electromagn. Soc. J.*, vol. 34, no. 5, pp. 799-806, 2019.
- [6] H. Wakatsuchi, D. F. Sievenpiper, and C. Christopoulos, "Designing flexible and versatile metamaterial absorbers," *IEEE Electromagn. Compat. Mag.*, vol. 5, no. 2, pp. 76-82, 2016.
- [7] X. Lu, J. Chen, Y. Huang, Z. Wu, and A. Zhang, "Design of ultra-wideband and transparent absorber based on resistive films," *Appl. Comput. Electromagn. Soc. J.*, vol. 34, no. 5, pp. 765-770, 2019.
- [8] Y. Ozturk and A. E. Yilmaz, "Multiband and perfect absorber with circular fishnet metamaterial and its variations," *Appl. Comput. Electromagn. Soc. J.*, vol. 31, no. 12, pp. 1445-1451, 2016.
- [9] P. Zhou, Q. Huang, L. Ji, and X. Shi, "Design of a thin broadband metamaterial absorber based on resistance frequency selective surface," *Appl. Comput. Electromagn. Soc. J.*, vol. 37, no. 10, pp. 1494-1499, 2019.
- [10] S. I. Rosaline and S. Raghavan, "Metamaterial-inspired split ring monopole antenna for WLAN applications," *Appl. Comput. Electromagn. Soc. J.*, vol. 33, no. 2, pp. 188-191, 2018.
- [11] K. Yu, Y. Li, and X. Liu, "Mutual coupling reduction of a MIMO antenna array using 3-D novel meta-material structures," *Appl. Comput. Electromagn. Soc. J.*, vol. 33, no. 7, pp. 758-763, 2018.
- [12] M. F. Finch and B. A. Lail, "A subwavelength perfect absorbing metamaterial patch array coupled with a molecular resonance," *Appl. Comput. Electromagn. Soc. J.*, vol. 33, no. 2, pp. 196-199, 2018.
- [13] M. Valayil and K. Chamberlin, "Enhancement of parameters of slotted waveguide antennas using metamaterials," *Appl. Comput. Electromagn. Soc. J.*, vol. 34, no. 2, pp. 272-279, 2019.
- [14] S. Luo, Y. Li, Y. Xia, and L. Zhang, "A low mutual coupling antenna array with gain enhancement using metamaterial loading and neutralization line structure," *Appl. Comput. Electromagn. Soc. J.*, vol. 34, no. 3, pp. 411-418, 2019.
- [15] S. Luo, Y. Li, Y. Xia, G. Yang, L. Sun, and L. Zhao, "Mutual coupling reduction of a dual-band antenna array using dual-frequency metamaterial structure," *Appl. Comput. Electromagn. Soc. J.*, vol. 34, no. 3, pp. 403-410, 2019.
- [16] H. R. Vani, M. A. Goutham, and Paramesha, "Gain enhancement of microstrip patch antenna using metamaterial superstrate," *Appl. Comput. Electromagn. Soc. J.*, vol. 34, no. 5, pp. 823-826, 2019.
- [17] A. Mersani, O. Lotfi, and J.-M. Ribero, "Design of a textile antenna with artificial magnetic conductor for wearable applications," *Microw. Opt. Technol. Lett.*, vol. 60, no. 6, pp. 1343-1349, Jun. 2018.
- [18] S. Can and A. E. Yilmaz, "Radar cross section reduction of a plate with textile-based single negative metamaterial," *2016 10th Eur. Conf. Antennas Propagation, EuCAP 2016*, pp. 1-4, 2016.
- [19] M. A. A. Abessolo, Y. Diallo, A. Jaoujal, A. E. Moussaoui, and N. Aknin, "Stop-band filter using a new metamaterial complementary split triangle resonators (CSTRs)," *Appl. Comput. Electromagn. Soc. J.*, vol. 28, no. 4, pp. 353-358, 2013.
- [20] M. E. Jalil, N. A. Samsuri, M. K. A. Rahim, and R. Dewan, "Compact chipless RFID metamaterial based structure using textile material," *2015 International Symposium on Antennas and Propagation (ISAP)*, pp. 5-8, 2015.
- [21] S. Lai, Y. Wu, X. Zhu, W. Gu, and W. Wu, "An optically transparent ultrabroadband microwave absorber," *IEEE Photonics J.*, vol. 9, no. 6, pp. 1-10, Dec. 2017.
- [22] M. Ghebrebrhan, *et al.*, "Textile frequency selective surface," *IEEE Microw. Wirel. Components Lett.*, vol. 27, no. 11, pp. 989-991, 2017.
- [23] Y. Zhang, J. Duan, B. Zhang, W. Zhang, and W. Wang, "A flexible metamaterial absorber with four bands and two resonators," *J. Alloys Compd.*, vol. 705, pp. 262-268, 2017.
- [24] K. Ling, K. Kim, and S. Lim, "Flexible liquid metal-filled metamaterial absorber on polydimethylsiloxane (PDMS)," *Opt. Express*, vol. 23, no. 16, pp. 21375, 2015.
- [25] R. Yahiaoui, S. Tan, L. Cong, R. Singh, F. Yan, and W. Zhang, "Multispectral terahertz sensing with highly flexible ultrathin metamaterial absorber," *J. Appl. Phys.*, vol. 118, no. 8, 2015.
- [26] H. K. Kim, K. Ling, K. Kim, and S. Lim, "Flexible inkjet-printed metamaterial absorber for coating a cylindrical object," *Opt. Express*, vol. 23, no. 5, pp. 5898, 2015.
- [27] H.-M. Lee, "A broadband flexible metamaterial absorber based on double resonance," *Prog. Electromagn. Res. Lett.*, vol. 46, pp. 73-78, Mar. 2014.
- [28] M. Nasr, *et al.*, "Narrowband metamaterial absorber for terahertz secure labeling," *J. Infrared, Millimeter, Terahertz Waves*, vol. 38, no. 9, pp. 1120-1129, 2017.
- [29] X. Kong, J. Xu, J. jun Mo, and S. Liu, "Broadband and conformal metamaterial absorber," *Front. Optoelectron.*, vol. 10, no. 2, pp. 124-131, 2017.
- [30] X. Yan, L.-J. Liang, X. Ding, and J.-Q. Yao, "Solid analyte and aqueous solutions sensing based on a flexible terahertz dual-band metamaterial

- absorber,” *Opt. Eng.*, vol. 56, no. 2, pp. 027104, 2017.
- [31] J. H. Kim, *et al.*, “Investigation of robust flexible conformal THz perfect metamaterial absorber,” *Appl. Phys. A Mater. Sci. Process.*, vol. 122, no. 4, pp. 1-7, 2016.
- [32] Y. He, *et al.*, “Optically-controlled metamaterial absorber based on hybrid structure,” *Opt. Commun.*, vol. 356, pp. 595-598, 2015.
- [33] M. Michalak, R. Brazis, V. Kazakevicius, J. Bilska, and I. Krucinska, “Novel approach to textile design for barriers against electromagnetic radiation,” *Int. J. Mater. Prod. Technol.*, vol. 36, no. 1/2/3/4, pp. 166, 2010.
- [34] P. Pa, M. S. Mirotznik, R. McCauley, S. Yarlagadda, and K. Duncan, “Integrating metamaterials within a structural composite using additive manufacturing methods,” *IEEE Antennas Propag. Soc. AP-S Int. Symp.*, pp. 0-1, 2012.
- [35] S. Can, A. E. Yilmaz, and E. Karakaya, “Conformal dual-band frequency selective surface on textile: design, prototyping and experiment,” *2017 Usn. Radio Sci. Meet. (Joint with AP-S Symp. Usn. 2017)*, pp. 17-18, 2017.
- [36] C. Huppé, *et al.*, “Woven metamaterials with an electromagnetic phase-advance for selective shielding,” *IOP Conf. Ser. Mater. Sci. Eng.*, vol. 254, no. 3, 2017.
- [37] D. Lee and S. Lim, “Wearable metamaterial absorber using screen printed channel logo,” *Int. Symp. Antennas Propag.*, pp. 928-929, 2016.
- [38] J. Tak and J. Choi, “A wearable metamaterial microwave absorber,” *IEEE Antennas Wirel. Propag. Lett.*, vol. 16, pp. 784-787, 2017.
- [39] G. A. Cavalcante, A. G. D’Assunção, and A. G. D’Assunção, “An iterative full-wave method for designing bandstop frequency selective surfaces on textile substrates,” *Microw. Opt. Technol. Lett.*, vol. 56, no. 2, pp. 383-388, Feb. 2014.
- [40] H. İbili, B. Karaosmanoğlu, and Ö. Ergül, “Demonstration of negative refractive index with low-cost inkjet-printed microwave metamaterials,” *Microw. Opt. Technol. Lett.*, vol. 60, no. 1, pp. 187-191, 2018.
- [41] R. Abdulla, E. Delihasanlar, F. G. Kizilcay Abdulla, and A. H. Yuzer, “Electromagnetic shielding characterization of conductive knitted fabrics,” *Prog. Electromagn. Res. M*, vol. 56, pp. 33-41, Jan. 2017.
- [42] S. J. Orfanidis, *Electromagnetic Waves and Antennas*, Rutgers University New Brunswick, NJ, 2002.
- [43] T. S. Nutting and G. A. V. Leaf, “5-A generalized geometry of weft-knitted fabrics,” *J. Text. Inst. Trans.*, vol. 55, no. 1, pp. T45-T53, Jan. 1964.
- [44] T. M. McBride and J. Chen, “Unit-cell geometry in plain-weave fabrics during shear deformations,” *Compos. Sci. Technol.*, vol. 57, no. 3, pp. 345-351, 1997.



**Ediz Delihasanlar** received an Electronics and Communication Engineering degree from the Suleyman Demirel University and a Master’s degree from Karabuk University, Turkey. He is a Research Assistant of Electrical-Electronics Engineering at the Karabuk University. His current research interests include metamaterials, applied electromagnetic, wave propagations, and dielectric constant.



**Ahmet Hayrettin Yuzer** received his B.Sc. and M.Sc. degrees in Electrical and Electronics Engineering from Inonu University, Malatya, Turkey, in 1995 and 2002, respectively and his Ph.D. degree in Electrical and Electronics Engineering in 2011 from Middle East Technical University (METU), Ankara, Turkey. He worked as a Research Assistant from 1999 to 2002 at Inonu University and from 2002 to 2011 at METU. He was at the Intelligent RF Radio Laboratory (iRadio Lab), University of Calgary, Calgary, Canada, as a visiting Ph.D. student from Sept. 2010 to Mar. 2011. Since 2011, he has been an Assistant Professor with the Department of Electrical and Electronics Engineering at Karabuk University, Karabuk, Turkey. His current scientific research includes amplifier modeling, measurement, linearization, and active and passive microwave components. Yuzer has been given a URSI 2008 Student Paper Contest award.